

A variational frequency-dependent stabilization for the Helmholtz equation with noisy Cauchy data

Vo Anh Khoa^{a,*}, Nguyen Dat Thuc^b, Ajith Gunaratne^a

^a*Department of Mathematics, Florida A&M University, Tallahassee, FL 32307, USA*

^b*Department of Mathematics and Computer Science, VNUHCM-University of Science, Ho Chi Minh City, Vietnam*

Abstract

This article considers a Cauchy problem of Helmholtz equations whose solution is well known to be exponentially unstable with respect to the inputs. In the framework of variational quasi-reversibility method, a Fourier truncation is applied to appropriately perturb the underlying problem, which allows us to obtain a stable approximate solution. Unlike the original version of the truncation, our perturbation is driven by the frequencies, rather than the noise level. This deals with real-world circumstances that one only measures data once or even does not know the noise level in advance, but needs to truncate high Fourier frequencies appropriately. The corresponding approximate problem is of a hyperbolic equation, which is also a crucial aspect of this approach. Error estimate between the approximate and true solutions is derived with respect to the noise level and to the frequencies is derived. From this analysis, the Lipschitz stability with respect to the noise level follows. Some numerical examples are provided to see how our numerical algorithm works well.

Keywords: Stabilization, Helmholtz equation, Ill-posed problems, Convergence, Error estimate

2010 MSC: 65J05, 65J20, 35K92

1. Statement of the Cauchy problem

In this work, we are concerned with the reconstruction problem of electromagnetic field from its knowledge on a part of boundary of the physical region Ω . Here, $\Omega = (0, 1) \times (0, 1)$ is our computational domain of interest, but it can be extended easily to $(0, a_1) \times (0, a_2)$, where a_1, a_2 are two positive numbers. Often, the propagation of the electromagnetic wave field is governed by the system of the Maxwell's equations for the electric field $\mathbf{E} = \mathbf{E}(x, y, t)$ and the magnetic field $\mathbf{B} = \mathbf{B}(x, y, t)$. Considering Ω as a homogeneous medium in a region with free currents and charges, this system can be reduced to the classical wave equations, cf. [1],

$$\frac{\partial^2 \mathbf{E}}{\partial t^2} - c^2 \Delta \mathbf{E} = 0, \quad \frac{\partial^2 \mathbf{B}}{\partial t^2} - c^2 \Delta \mathbf{B} = 0 \quad \text{in } \Omega \times (0, T), \quad (1)$$

where $c > 0$ is the speed of light and $T > 0$ is the travel time. Consider the frequency $\omega > 0$. For $i = \sqrt{-1}$, we take $\mathbf{E}(x, y, t) = e^{i\omega t} \mathbf{E}(x, y)$ and $\mathbf{B}(x, y, t) = e^{i\omega t} \mathbf{B}(x, y)$. Then, setting $k = \omega/c > 0$, it follows from system (1) that

$$\Delta \mathbf{E}(x, y) + k^2 \mathbf{E}(x, y) = 0, \quad \Delta \mathbf{B}(x, y) + k^2 \mathbf{B}(x, y) = 0, \quad (2)$$

which form a system of Helmholtz equations. Since system (2) is uncoupled and linear with respect to each component of $\mathbf{E}(x, y)$ and $\mathbf{B}(x, y)$, it is pertinent to solve the following model:

$$\Delta u(x, y) + k^2 u(x, y) = 0 \quad \text{in } \Omega. \quad (3)$$

Note that in (2), $\mathbf{E}(x, y)$ and $\mathbf{B}(x, y)$ are complex-valued components, but it is sufficient to find a real-valued function $u = u(x, y)$ in (3). Physically, fields vanish far from the axes and thus, we can assume that the electromagnetic field vanishes on the sides $\{y = 0\}$ and $\{y = 1\}$ of the computational domain Ω . Mathematically, we consider

$$u(x, 0) = u(x, 1) = 0 \quad \text{for } x \in (0, 1). \quad (4)$$

*This work was supported by the Faculty Research Awards Program (FRAP) at Florida A&M University, under the project "Approximation of a time-reversed reaction-diffusion system in cancer cell population dynamics" (007633).

*Corresponding author

Email address: anhkhao.vo@fam.u.edu (Vo Anh Khoa)

On the other hand, we assume to measure the electromagnetic Cauchy data at $\{x = 0\}$,

$$u(0, y) = u_0(y), \quad u_x(0, y) = u_1(y) \quad \text{for } y \in (0, 1). \quad (5)$$

Cf. [2], we remark that the second data (i.e. the Neumann data at $x = 0$) in (5) can be reduced to the zero boundary condition. In fact, let $U = U(x, y)$ be a solution to the following system:

$$\begin{cases} \Delta U(x, y) + k^2 U(x, y) = 0 & \text{in } \Omega, \\ U(x, 0) = U(x, 1) = 0 & \text{for } x \in (0, 1), \\ U_x(0, y) = u_1(y), U(1, y) = 0 & \text{for } y \in (0, 1). \end{cases} \quad (6)$$

Next, consider $V = V(x, y)$ as a solution to the following system:

$$\begin{cases} \Delta V(x, y) + k^2 V(x, y) = 0 & \text{in } \Omega, \\ V(x, 0) = V(x, 1) = 0 & \text{for } x \in (0, 1), \\ V(0, y) = u_0(y) - U(0, y), V_x(0, y) = 0 & \text{for } y \in (0, 1). \end{cases} \quad (7)$$

With (6) and (7), it is clear that the solution u to system (3)–(5) can be computed via $u = U + V$. By [2, Lemma 1], we know that system (6) is well-posed with U in $H^2(\Omega)$ when $u_1 \in L^2(0, 1)$ and thus, $U(0, y)$ exists in $H^2(0, 1)$ by the embedding $H^2(\Omega) \subset C([0, 1]; H^2(0, 1))$. Henceforth, from (7), instead of working on the Cauchy data (5) we can assume that $u_1 = 0$ in (5) in our analysis below.

Combining (3), (4) and (5) with $u_1 = 0$ forms our Cauchy problem for the Helmholtz equation. In this scenario, we want to reconstruct the whole wave field in Ω and especially, the field at the boundary $x = 1$.

Remark 1. Cf. the appendix of [3], if the incident electric wave field has only one non-zero component, then the propagation of this component in a heterogeneous medium is governed equally well by a single Helmholtz equation. In other words, the Helmholtz equation may play an equal role as the Maxwell's system when the medium is no longer homogeneous as assumed above.

2. Preliminary analysis and frequency-dependent stabilization

Let A be either a Banach space or a Hilbert space. We call A' the dual space of A . For a certain Banach space A , $\|\cdot\|_A$ stands for the A -norm. When A is Hilbert, we define the A -norm of u as $\|u\|_A^2 = \langle u, u \rangle_A$, where $\langle \cdot, \cdot \rangle_A$ is the corresponding inner product. Throughout the paper, we will use $\langle \cdot, \cdot \rangle$ to indicate either the scalar product in $L^2(0, 1)$ or the dual pairing of a continuous linear functional and an element of a function space. We thereby denote by $\|\cdot\|$ the $L^2(0, 1)$ -norm.

The Cauchy problem of Helmholtz equation is well known to be unstable with respect to any small perturbation of the data. Based on the zero Dirichlet boundary condition (4), the Laplace operator $-\partial^2/\partial y^2$ is non-negative. According to the standard result for the Dirichlet eigenvalue problem, there exists an orthonormal basis $\{\phi_j\}$ of $L^2(0, 1)$ such that $\phi_j \in H^1(0, 1) \cap C^\infty[0, 1]$ and $-d^2/dy^2 \phi_j(y) = \mu_j \phi_j(y)$. The Dirichlet eigenvalues μ_j in this case form an infinite sequence such that $0 \leq \mu_0 < \mu_1 < \mu_2 < \dots$, and $\lim_{j \rightarrow \infty} \mu_j = \infty$. It follows from (3) and (5) that we obtain the following initial-value differential system:

$$\begin{cases} \frac{d^2}{dx^2} \langle u(x, \cdot), \phi_j \rangle - \lambda_{j,k} \langle u(x, \cdot), \phi_j \rangle = 0, \\ \langle u(0, \cdot), \phi_j \rangle = \langle u_0, \phi_j \rangle, \quad \frac{d}{dx} \langle u(0, \cdot), \phi_j \rangle = 0. \end{cases} \quad (8)$$

In (8), $\lambda_{j,k} = \mu_j - k^2$. By this way, we solve system (8) in each of the following set of Fourier frequencies:

$$A_1 := \{j \in \mathbb{N} : \lambda_{j,k} > 0\}, \quad A_2 := \{j \in \mathbb{N} : \lambda_{j,k} = 0\}, \quad A_3 := \{j \in \mathbb{N} : \lambda_{j,k} < 0\}.$$

It is also straightforward to see that $\phi_j(y) = \sqrt{2} \sin(j\pi y)$, $\mu_j = j^2\pi^2$. In addition, $\{\phi'_j/\sqrt{\mu_j}\}_{j \in \mathbb{N}^*}$ is an orthonormal basis of $L^2(0, 1)$. Therefore, it holds that

$$\|u_y\|^2 = \sum_{j \in \mathbb{N}^*} \left| \left\langle u_y, \frac{\phi'_j}{\sqrt{\mu_j}} \right\rangle \right|^2 = \sum_{j \in \mathbb{N}^*} \left| \left\langle u, \frac{\phi''_j}{\sqrt{\mu_j}} \right\rangle \right|^2 = \sum_{j \in \mathbb{N}^*} \mu_j |\langle u, \phi_j \rangle|^2. \quad (9)$$

Theorem 1. The Fourier coefficient $\langle u(x, \cdot), \phi_j \rangle$ has the form:

$$\langle u(x, \cdot), \phi_j \rangle = \begin{cases} \cosh(\sqrt{\lambda_{j,k}}x) \langle u_0, \phi_j \rangle & \text{in } A_1, \\ \cos(\sqrt{-\lambda_{j,k}}x) \langle u_0, \phi_j \rangle & \text{in } A_3. \end{cases} \quad (10)$$

Proof. Proof of the theorem can be proceeded as in [2]. \square

Now, we show a very important relation of these Fourier frequencies in the following theorem.

Theorem 2. *Taking into account set A_1 , the Fourier coefficient of u satisfies the following relation:*

$$\lambda_{j,k} e^{(1-x)\sqrt{\lambda_{j,k}}} \left(\langle u(x, \cdot), \phi_j \rangle + \frac{1}{\sqrt{\lambda_{j,k}}} \langle u_x(x, \cdot), \phi_j \rangle \right) = \lambda_{j,k} \langle u(1, \cdot), \phi_j \rangle + \sqrt{\lambda_{j,k}} \langle u_x(1, \cdot), \phi_j \rangle. \quad (11)$$

Proof. From (10), we can compute that

$$\frac{1}{\sqrt{\lambda_{j,k}}} \langle u_x(x, \cdot), \phi_j \rangle = \sinh \left(\sqrt{\lambda_{j,k}} x \right) \langle u_0, \phi_j \rangle. \quad (12)$$

Thus, we take $x = 1$ in (12) and in (10) and then combine the resulting formulations to obtain (11). We complete the proof of the theorem. \square

Practically, the data u_0 in (5) always contain noise of measurement. Therefore, we assume to have $u_0^\varepsilon \in H^1(0, 1)$ as the noisy data such that for $\varepsilon \in (0, 1)$,

$$\|u_0^\varepsilon - u_0\|_{H^1(0,1)} \leq \varepsilon. \quad (13)$$

By Theorem 1, our Cauchy problem is exponentially unstable in A_1 due to the natural growth of the hyperbolic cosine function. Any small perturbation of the initial data u_0 may cause a huge error when computing solution u of the Cauchy problem. In this work, we then adapt our recent modified quasi-reversibility method (cf. [4] for elliptic operators and [5] for parabolic operators) to solve our system (3)–(5). To do so, we rewrite (3) as

$$u_{xx} - u_{yy} + 2u_{yy} + k^2 u = 0. \quad (14)$$

We then perturb (14) by a linear mapping \mathbf{Q} and take $\mathbf{P} = \mathbf{Q} + 2\partial^2/\partial y^2$. Henceforth, we arrive at

$$u_{xx} - u_{yy} + \mathbf{P}u + k^2 u = 0 \quad \text{in } \Omega. \quad (15)$$

It is worth mentioning that together with the boundary condition (4) and the Cauchy data (5) with measurement u_0^ε , (15) forms a system of wave equation. Herewith, x becomes a parametric time variable. Since the noise level ε is involved, we then seek a sequence of $\{u^\varepsilon\}_{\varepsilon>0}$ satisfying the following system:

$$\begin{cases} u_{xx}^\varepsilon - u_{yy}^\varepsilon + \mathbf{P}u^\varepsilon + k^2 u^\varepsilon = 0 & \text{in } \Omega, \\ u^\varepsilon(x, 0) = u^\varepsilon(x, 1) = 0 & \text{for } x \in (0, 1), \\ u^\varepsilon(0, y) = u_0^\varepsilon(y), \quad u_x^\varepsilon(0, y) = 0 & \text{for } y \in (0, 1). \end{cases} \quad (16)$$

Cf. [4, 5], \mathbf{Q} is called *perturbation* as it is to “absorb” high Fourier frequencies in the Laplace operator, and \mathbf{P} is called *stabilized operator* as it only contains large enough Fourier frequencies serving for the convergence of the scheme. Let $\gamma > 1$. Consider $B := \{j \in A_1 : \lambda_{j,k} > \log^2(\gamma)\}$. We choose the following truncation operator:

$$\mathbf{Q}u(x, \cdot) = 2 \sum_{j \in B} \lambda_{j,k} \langle u(x, \cdot), \phi_j \rangle \phi_j + 2 \sum_{j \in A_3} \lambda_{j,k} \langle u(x, \cdot), \phi_j \rangle \phi_j := \mathbf{Q}_1 u(x, \cdot) + \mathbf{Q}_2 u(x, \cdot). \quad (17)$$

As to the corresponding stabilized operator \mathbf{P} , we find that

$$\begin{aligned} \mathbf{P}u(x, \cdot) &= 2 \sum_{j \in B \cup A_3} \lambda_{j,k} \langle u(x, \cdot), \phi_j \rangle \phi_j - 2 \sum_{j \in \mathbb{N}} \mu_j \langle u(x, \cdot), \phi_j \rangle \phi_j \\ &= 2 \sum_{j \in B \cup A_3} (\lambda_{j,k} - \mu_j) \langle u(x, \cdot), \phi_j \rangle \phi_j - 2 \sum_{j \in \mathbb{N} \setminus (B \cup A_3)} \mu_j \langle u(x, \cdot), \phi_j \rangle \phi_j \\ &= -2k^2 \sum_{j \in \mathbb{N}} \langle u(x, \cdot), \phi_j \rangle \phi_j - 2 \sum_{j \in \mathbb{N} \setminus (B \cup A_3)} \lambda_{j,k} \langle u(x, \cdot), \phi_j \rangle \phi_j. \end{aligned}$$

Remark 2. Many works concerning the conventional truncation method (see, e.g., [4, 6, 7, 8, 9]) require the noise dependence to prove the strong convergence of the truncation projection in different physical models. However, practically we cannot know exactly the noise level or, if that noise is known, it is only measured once. Thus, it is reasonable to get another way to truncate high Fourier frequencies appropriately. We cannot truncate them arbitrarily due to the natural severe ill-posedness of the problem. In the present work, the frequency-dependent truncation is proposed, which is our novelty here. Since the wavenumber k is large in several physical applications; see our brief discussion after Theorem 4, we can, in fact, exploit this largeness to prove the error estimate of the scheme. By that way, we can obtain a stable approximation for the Cauchy problem.

In view of Parseval's identity, we now estimate that

$$\|\mathbf{Q}_1 u(x, \cdot)\|^2 = 4 \sum_{j \in B} e^{-2\sqrt{\lambda_{j,k}}} \lambda_{j,k}^2 e^{2\sqrt{\lambda_{j,k}}} |\langle u(x, \cdot), \phi_j \rangle|^2 \leq 4\gamma^{-2} \sum_{j \in B} \lambda_{j,k}^2 e^{2\sqrt{\lambda_{j,k}}} |\langle u(x, \cdot), \phi_j \rangle|^2. \quad (18)$$

By using (11) obtained in Theorem 2, we have

$$\begin{aligned} & \sup_{x \in [0,1]} \sum_{j \in B} \lambda_{j,k}^2 e^{2\sqrt{\lambda_{j,k}}} |\langle u(x, \cdot), \phi_j \rangle|^2 \\ & \leq \sup_{x \in [0,1]} \left[\sum_{j \in B} \lambda_{j,k}^2 e^{2(1-x)\sqrt{\lambda_{j,k}}} \left(\langle u(x, \cdot), \phi_j \rangle + \frac{1}{\sqrt{\lambda_{j,k}}} \langle u_x(x, \cdot), \phi_j \rangle \right)^2 \right] \\ & \leq \sum_{j \in B} \left(\lambda_{j,k} \langle u(1, \cdot), \phi_j \rangle + \sqrt{\lambda_{j,k}} \langle u_x(1, \cdot), \phi_j \rangle \right)^2 \leq 2 \|u(1, \cdot)\|_{H^2(0,1)}^2 + 2 \|u_x(1, \cdot)\|_{H^1(0,1)}^2. \end{aligned}$$

by means of $\langle u(x, \cdot), \phi_j \rangle \langle u_x(x, \cdot), \phi_j \rangle \geq 0$; cf. (10) and (12). Now we estimate $\mathbf{Q}_2 u$ as follows. Observe that if $\log(\gamma) \geq k$, then $\mu_i - k^2 \geq k^2 - \mu_j > 0$ for $i \in B$ and $j \in A_3$. This means that $\lambda_{i,k} \geq |\lambda_{j,k}|$ for $i \in B$ and $j \in A_3$. Therefore, we estimate that

$$\|\mathbf{Q}_2 u(x, \cdot)\|^2 = 4 \sum_{j \in A_3} |\lambda_{j,k}|^2 |\langle u(x, \cdot), \phi_j \rangle|^2 \leq 4 \sum_{j \in B} |\lambda_{j,k}|^2 |\langle u(x, \cdot), \phi_j \rangle|^2 = \|\mathbf{Q}_1 u(x, \cdot)\|^2. \quad (19)$$

Henceforth, we can assume that the true solution satisfies $u(1, \cdot) \in H^2(0, 1)$ and $u_x(1, \cdot) \in H^1(0, 1)$ to gain the strong convergence of the scheme. Note now that we can rewrite \mathbf{P} as

$$\mathbf{P}u(x, \cdot) = -2k^2 u(x, \cdot) - 2 \sum_{j \in \mathbb{N} \setminus (B \cup A_3)} \lambda_{j,k} \langle u(x, \cdot), \phi_j \rangle \phi_j \quad (20)$$

which is computable for our numerical simulation. Moreover, since in $\mathbb{N} \setminus (B \cup A_3)$ it holds that $0 \leq \lambda_{j,k} \leq \log^2(\gamma)$, we, according to Parseval's identity and using (9), get that

$$\|\mathbf{P}u(x, \cdot)\|^2 \leq 4k^4 \|u(x, \cdot)\|^2 + 4\log^2(\gamma) \|u_y(x, \cdot)\|^2. \quad (21)$$

3. Convergence analysis

We now formulate theorems for our convergence analysis. Existence and uniqueness theorems can be proven similarly to those theoretical findings in [4]. Therefore, we only state those theorems below without giving any proof.

Definition 1 (Weak solution). *For each $\varepsilon > 0$, a function $u^\varepsilon : [0, 1] \rightarrow H_0^1(0, 1)$ is said to be a weak solution to system (16) if*

- $u^\varepsilon \in C([0, 1]; H_0^1(0, 1))$, $\partial_x u^\varepsilon \in C([0, 1]; L^2(0, 1))$, $\partial_{x^2}^2 u^\varepsilon \in L^2(0, 1; (H^1(0, 1))')$;
- For every test function $\psi \in H_0^1(0, 1)$, it holds that

$$\left\langle \frac{\partial^2 u^\varepsilon}{\partial x^2}, \psi \right\rangle + \left\langle \frac{\partial u^\varepsilon}{\partial y}, \frac{\partial \psi}{\partial y} \right\rangle + \langle \mathbf{P}u^\varepsilon, \psi \rangle + k^2 \langle u^\varepsilon, \psi \rangle = 0 \quad \text{for a.e. in } (0, 1); \quad (22)$$

- $u^\varepsilon(0) = u_0^\varepsilon \in H^1(0, 1)$, $\partial_x u^\varepsilon(0) = 0$.

Theorem 3 (Existence and uniqueness of a weak solution). *For any $\varepsilon > 0$, system (16) admits a unique weak solution in the sense of Definition 1. Moreover, it holds that $u^\varepsilon \in C([0, 1]; H_0^1(0, 1))$ and $\partial_x u^\varepsilon \in C([0, 1]; L^2(0, 1))$.*

Theorem 4 (Error estimate). *Let $u \in C([0, 1]; H^2(0, 1)) \cap C^1([0, 1]; H^1(0, 1))$ be a unique solution of the Cauchy problem of (3)–(5). Let $M > 0$ independent of ε and k be such that $\|u\|_{C([0,1]; H^2(0,1)) \cap C^1([0,1]; H^1(0,1))} \leq M$. Let u^ε be a unique weak solution of system (16) as analyzed in Theorem 3. Then, by choosing $\log(\gamma) = 2k - \eta$ for $0 < \eta \leq k$, the following L^2 error estimate holds:*

$$\|u^\varepsilon(x, \cdot) - u(x, \cdot)\|^2 \leq \left(\frac{1}{k^2} + 1 \right) \varepsilon^2 e^{(4k+1)x} + \frac{16M^2 e^{4k(x-1)+2\eta+x}}{k^2}. \quad (23)$$

Proof. Consider the difference function $w = u^\varepsilon - u$. It is straightforward that this function satisfies the corresponding difference equation:

$$w_{xx} - w_{yy} + k^2 w = -\mathbf{P}w + \mathbf{Q}u \quad \text{in } \Omega. \quad (24)$$

Besides, this equation is associated with the Dirichlet boundary condition and the initial conditions

$$\begin{cases} w(x, 0) = w(x, 1) = 0 & \text{for } x \in (0, 1), \\ w(0, y) = u_0^\varepsilon(y) - u_0(y), \quad w_x(0, y) = 0 & \text{for } y \in (0, 1). \end{cases} \quad (25)$$

Multiply both sides of (24) by w_x and integrate the resulting equation with respect to y from 0 to 1. After that, dividing both sides of the resulting equation by k^2 gives

$$\frac{1}{k^2} \frac{d}{dx} \|w_x(x, \cdot)\|^2 + \frac{1}{k^2} \frac{d}{dx} \|w_y(x, \cdot)\|^2 + \frac{d}{dx} \|w(x, \cdot)\|^2 = \frac{2}{k^2} \langle \mathbf{Q}u(x, \cdot), w_x(x, \cdot) \rangle - \frac{2}{k^2} \langle \mathbf{P}w(x, \cdot), w_x(x, \cdot) \rangle.$$

Using the energy estimate (21) of the stabilized operator in combination of the Cauchy–Schwarz inequality, we estimate that

$$\begin{aligned} -\frac{2}{k^2} \langle \mathbf{P}w(x, \cdot), w_x(x, \cdot) \rangle &\leq \frac{1}{k^2} \left[\frac{1}{4k} \|\mathbf{P}w(x, \cdot)\|^2 + 4k \|w_x(x, \cdot)\|^2 \right] \\ &\leq \frac{k^4}{k^3} \|w(x, \cdot)\|^2 + \frac{\log^2(\gamma)}{k^3} \|w_y(x, \cdot)\|^2 + \frac{4}{k} \|w_x(x, \cdot)\|^2 \end{aligned}$$

In the same vein, using (17), (18) and (19), we obtain the following estimate:

$$\frac{2}{k^2} \langle \mathbf{Q}_\varepsilon u(x, \cdot), w_x(x, \cdot) \rangle \leq \frac{16\gamma^{-2}}{k^2} \|u\|_{C([0,1]; H^2(0,1)) \cap C^1([0,1]; H^1(0,1))}^2 + \frac{1}{k^2} \|w_x(x, \cdot)\|^2$$

Therefore, $\log(\gamma) = 2k - \eta$ where $0 < \eta \leq k$, we have

$$\begin{aligned} &\frac{1}{k^2} \frac{d}{dx} \|w_x(x, \cdot)\|^2 + \frac{1}{k^2} \frac{d}{dx} \|w_y(x, \cdot)\|^2 + \frac{d}{dx} \|w(x, \cdot)\|^2 \\ &\leq \frac{16\gamma^{-2}}{k^2} M^2 + \frac{4k+1}{k^2} \|w_x(x, \cdot)\|^2 + k \|w(x, \cdot)\|^2 + \frac{\log^2(\gamma)}{k^3} \|w_y(x, \cdot)\|^2 \\ &\leq \frac{16e^{-4k+2\eta}}{k^2} M^2 + \frac{4k+1}{k^2} \|w_x(x, \cdot)\|^2 + k \|w(x, \cdot)\|^2 + \frac{(2k-\eta)^2}{k^3} \|w_y(x, \cdot)\|^2 \end{aligned}$$

By Gronwall's inequality and using (13) and (25), we, after dropping the gradient norms on the left-hand side, find that

$$\begin{aligned} \|w(x, \cdot)\|^2 &\leq \left(\frac{1}{k^2} \|w_x(0, \cdot)\|^2 + \frac{1}{k^2} \|w_y(0, \cdot)\|^2 + \|w(0, \cdot)\|^2 + \frac{16M^2 e^{-4k+2\eta} x}{k^2} \right) e^{(4k+1)x} \\ &\leq \left[\left(\frac{1}{k^2} + 1 \right) \varepsilon^2 + \frac{16M^2 e^{-4k+2\eta} x}{k^2} \right] e^{(4k+1)x}. \end{aligned}$$

This completes the proof of the theorem. \square

From (23) in Theorem 4, if we only measure the data once, i.e. only one $\varepsilon \in (0, 1)$ is attained, then we can still obtain a fine approximation to u by collecting data for a set of multiple high frequencies. In this case, we consider $\underline{k} \leq k \leq \bar{k}$, where $\underline{k} > 1$, and thus, $u(x, y)$ solutions to the Cauchy problem is understood as $u(x, y, k)$. The perspective of multiple frequencies is relevant to the inverse scattering problem for detection of suspicious explosive-like objects; cf. e.g. [10], when the near-field scattering is approximated by the far-field measurement. Moreover, as practically shown in [10, 11], the wavenumber k is large. Now, assume ε fixed such that $\bar{k}^2 e^{4\bar{k}} \leq K\varepsilon^{-2}$ for $K > 0$, then u^ε is close to u in L^2 sense with an error of $\mathcal{O}(k^{-2})$.

Similarly, if we fix a set of k such that $4k \geq K \log(\varepsilon^{-\alpha})$ for $\alpha > 0$ and $K > 0$, then u^ε is close to u in L^2 sense with an error of $\mathcal{O}(\varepsilon^{\min\{\alpha, 2\}})$. It is also easy to deduce from the above proof that we can obtain a Lipschitz stability of the scheme in terms of ε , as \mathbf{Q} is not involved.

4. Numerical examples

Given $M, N \in \mathbb{N}$, we consider uniform grids of mesh-points $x_m = m\Delta x, y_n = n\Delta y$ for $m \leq M, n \leq N$ with $\Delta x, \Delta y$ being the mesh-widths in x and y , respectively. For any function $u(x, y)$, we denote by $u_{m,n} \approx u(x_m, y_n)$ the corresponding discrete function. To generate the data, we apply the central finite difference method (FDM) to solve the Helmholtz equation (3) with the Dirichlet boundary conditions imposed on four sides of $\Omega = [0, 1]^2$, viz.

$$u(0, y) = u_0(y), \quad u(1, y) = g(y), \quad u(x, 0) = 0, \quad u(x, 1) = 0. \quad (26)$$

In our numerical performance of the stabilization scheme below, we do not choose the true solution of the Helmholtz equation (3). Instead, we choose its boundary data u_0, g in (26) so that our choice is more flexible. This is relevant because (3) with full data (26) is a well-posed problem and the central FDM is well known to be stable and convergent with respect to the refinement of x and y . In this circumstance, one can consider the discrete function $u_{m,n}$ obtained from that well-posed problem as a reliable true solution. The Neumann data u_1 in (5) can be generated using the fact that

$$u_0(y_n) \approx u_1(y_n)\Delta x + u(x_1, y_n).$$

The same FDM is applied when we solve $U(x, y)$ of system (6). Thereby, a stable approximation of $U(0, y)$ can be obtained for the Dirichlet data in (7). To solve for $V(x, y)$ in (7) numerically, we remark that the stabilized operator \mathbf{P} (cf. (20)) needs to be linearized, albeit it is a linear mapping. Cf. [4] and based on (16), the linearized stabilized problem for (7) is established as follows. We construct a sequence of $\{V^{\varepsilon, q}\}_{q \in \mathbb{N}}$ satisfying

$$\begin{cases} V_{xx}^{\varepsilon, q+1} - V_{yy}^{\varepsilon, q+1} + \mathbf{P}_1 V^{\varepsilon, q} - k^2 V^{\varepsilon, q+1} = 0 & \text{in } \Omega, \\ V^{\varepsilon, q+1}(x, 0) = V^{\varepsilon, q+1}(x, 1) = 0 & \text{for } x \in (0, 1), \\ V^{\varepsilon, q+1}(0, y) = u_0^\varepsilon(y) - U(0, y), \quad V_x^{\varepsilon, q+1}(0, y) = 0 & \text{for } y \in (0, 1). \end{cases} \quad (27)$$

In (27), we use

$$\mathbf{P}_1 u(x, \cdot) = -2 \sum_{j \in \mathbb{N} \setminus (B \cup A_3)} \lambda_{j,k} \langle u(x, \cdot), \phi_j \rangle \phi_j,$$

and the initial guess $V^{\varepsilon, 0}$ (i.e. $q = 0$) is chosen to be $u_0^\varepsilon(y) - U(0, y)$. We choose this initial guess because it is a unique function that contains many information of our sought V^ε under stabilization. As to the measured data u_0^ε , we apply the additive noise in the following sense: $u_0^\varepsilon(y) = u_0(y) + \varepsilon \text{rand}(y)$, where rand is a uniformly distributed random number such that $\max_{y \in [0, 1]} |\text{rand}(y)| \leq 1$. At the discretization level, the gradient of u_0^ε is then approximated by

$$\partial_y u_0^\varepsilon(y_n) \approx \frac{u_0^\varepsilon(y_{n+1}) - u_0^\varepsilon(y_n)}{\Delta y} \approx \partial_y u_0(y_n) + \varepsilon N (\text{rand}(y_{n+1}) - \text{rand}(y_n)).$$

Therefore, we can see that to fulfill assumption (13), having the measured data u_0^ε is practically sufficient if we choose N such that either $N \leq \varepsilon^{-\beta}$ or $N \leq k^\beta$ holds for $\beta \in (0, 1)$. Subsequently, a coarse mesh for the domain of y should be used.

For the (local) convergence of the linearization scheme for (27), we refer the reader to the pioneering work [4], where the same convergence analysis is studied. Since the convergence is local in x , we use a fine mesh for this variable. We do not detail how small Δx should be as it can be done as in [4]. Generally, it requires that $\log(\gamma)\Delta x\gamma^{\Delta x} < 1$.

For each iteration q , we apply the same central FDM to approximate $V^{\varepsilon, q}$. The inner product in \mathbf{P}_1 can be approximated by the standard Riemann sum. Henceforth, we can obtain the fully discrete version of (27) in matrix form. We refer the reader to [4] for the standard derivation of this form. Note that after having $V^{\varepsilon, q}$, we obtain an approximation of u^ε via $u_{m,n}^\varepsilon = U_{m,n} + V_{m,n}^{\varepsilon, q}$.

Now, in all examples below, we choose $\eta = k, M = 400, N = 80$ and $q = 1$. To show how good our proposed scheme is, all numerical results are reported with $\varepsilon = 0.99, 0.01$. Often, the noise level is not too small in practice. Moreover, it can be seen that our scheme is not much expensive as q is relatively small. Below, we consider the following relative error:

$$E = \frac{\sqrt{\sum_{m=0}^M \sum_{n=0}^N |u_{m,n}^\varepsilon - u_{m,n}|^2}}{\sqrt{\sum_{m=0}^M \sum_{n=0}^N |u_{m,n}|^2}} \times 100\%.$$

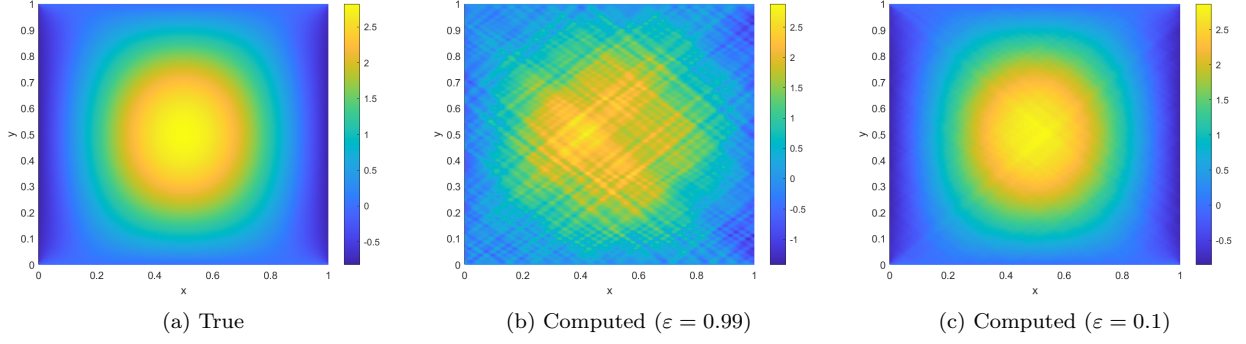


Figure 1: Numerical results of Example 1 (low-frequency problem). (a) Graphical illustration of the true solution. (b) and (c) Illustrations of the reconstructed solution with $\varepsilon = 0.99$ and $\varepsilon = 0.1$, respectively.

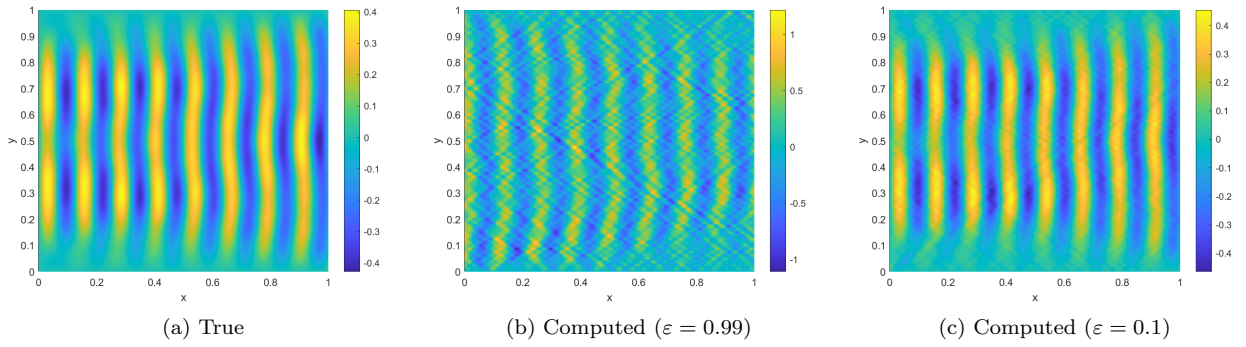


Figure 2: Numerical results of Example 1 (high-frequency problem). (a) Graphical illustration of the true solution. (b) and (c) Illustrations of the reconstructed solution with $\varepsilon = 0.99$ and $\varepsilon = 0.1$, respectively.

Example 1: Low frequency

In this test, we choose $k = 5$ and

$$u_0(y) = -e^{-2(0.5^4 + (y-0.5)^4)} + 0.5^4 + (y - 0.5)^4, \quad g(y) = u_0(y).$$

Such k is suitable in the context of landmine detection; cf. e.g. [10]. Depicted in Figure 1 are the graphical illustrations of the true solution and its reconstructed with large noise ($\varepsilon = 0.99$) and intermediate noise ($\varepsilon = 0.1$). When ε is smaller, the computed solution is very close to the true one in terms of the value and, furthermore, the shape and location of the yellow circular protrusion; see Figures 1a and 1c. On the other hand, the relative error reduces from 30.00% for $\varepsilon = 0.99$ to 1.91% for $\varepsilon = 0.1$, which shows the efficiency of the scheme. In this example, it is concrete that choosing a frequency-dependent stabilization works very well in the reconstruction process, compared to the noise-dependent choice in the previous works.

Example 2: High frequency

In this test, we consider $k = 50$ and

$$u_0(y) = 0, \quad g(y) = \frac{-\sin\left(7\sqrt{0.001 + (y - 0.5)^2}\right)}{7\sqrt{1 + (y - 0.5)^2}}.$$

Similar to Example 1, we can see the reconstruction becomes better when ε decreases from 0.99 to 0.1; see Figure 2. Especially, when $\varepsilon = 0.1$, the computed solution, cf. Figure 2c shows exactly the same shape and location of all yellow bands in the true solution (Figure 2). In Figure 2b for $\varepsilon = 0.99$, those bands do not have the correct shape. Moreover, the illustration when $\varepsilon = 0.1$ is much clearer than that of $\varepsilon = 0.99$. This observation is exactly the same as in Example 1; see Figures 1b and 1c. We also report that the relative error E in this case reduces significantly from 183.38% to 16.18%, when ε decreases from 0.99 to 0.1.

Acknowledgment

V.A.K. thanks Prof. Dr. Roselyn Williams (Tallahassee, USA) for her support during the time V.A.K. working at Florida A&M University.

References

- [1] M. Born, E. Wolf, Principles of Optics, Cambridge University Press, 2019.
- [2] N. H. Tuan, V. A. Khoa, M. N. Minh, T. Tran, Reconstruction of the electric field of the Helmholtz equation in three dimensions, *Journal of Computational and Applied Mathematics* 309 (2017) 56–78. doi:10.1016/j.cam.2016.05.021.
- [3] M. V. Klibanov, D.-L. Nguyen, L. H. Nguyen, A coefficient inverse problem with a single measurement of phaseless scattering data, *SIAM Journal on Applied Mathematics* 79 (1) (2019) 1–27. doi:10.1137/18m1168303.
- [4] V. A. Khoa, P. T. H. Nhan, Constructing a variational quasi-reversibility method for a Cauchy problem for elliptic equations, *Mathematical Methods in the Applied Sciences* 44 (5) (2020) 3334–3355. doi:10.1002/mma.6945.
- [5] H. T. Nguyen, V. A. Khoa, V. A. Vo, Analysis of a quasi-reversibility method for a terminal value quasi-linear parabolic problem with measurements, *SIAM Journal on Mathematical Analysis* 51 (1) (2019) 60–85. doi:10.1137/18m1174064.
- [6] P. T. Nam, D. D. Trong, N. H. Tuan, The truncation method for a two-dimensional nonhomogeneous backward heat problem, *Applied Mathematics and Computation* 216 (2010) 3423–3432.
- [7] T. Regińska, K. Regiński, Approximate solution of a Cauchy problem for the Helmholtz equation, *Inverse Problems* 22 (3) (2006) 975–989. doi:10.1088/0266-5611/22/3/015.
- [8] N. H. Tuan, L. D. Thang, V. A. Khoa, T. Tran, On an inverse boundary value problem of a nonlinear elliptic equation in three dimensions, *Journal of Mathematical Analysis and Applications* 426 (2015) 1232–1261.
- [9] N. H. Tuan, V. A. Khoa, P. T. K. Van, V. V. Au, An improved quasi-reversibility method for a terminal-boundary value multi-species model with white Gaussian noise, *Journal of Computational and Applied Mathematics* 384 (2021) 113176. doi:10.1016/j.cam.2020.113176.
- [10] V. A. Khoa, G. W. Bidney, M. V. Klibanov, L. H. Nguyen, L. H. Nguyen, A. J. Sullivan, V. N. Astratov, Convexification and experimental data for a 3D inverse scattering problem with the moving point source, *Inverse Problems* 36 (8) (2020) 085007. doi:10.1088/1361-6420/ab95aa.
- [11] V. L. R. Murthy, S. V. J. Lakshman, Electronic absorption spectrum of cobalt antipyrene complex, *Solid State Communications* 38 (7) (1981) 651–652. doi:10.1016/0038-1098(81)90960-1.